

Measuring Multi-Configurational Character by Orbital Entanglement

Christopher J. Stein and Markus Reiher^{a)}

ETH Zürich, Laboratorium für Physikalische Chemie, Vladimir-Prelog-Weg 2, 8093 Zürich, Switzerland

(Dated: 3 September 2022)

One of the most critical tasks at the very beginning of a quantum chemical investigation is the choice of either a multi- or single-configurational method. Naturally, many proposals exist to define a suitable diagnostic of the multi-configurational character for various types of wave functions in order to assist this crucial decision. Here, we present a new orbital-entanglement based multi-configurational diagnostic termed $Z_{s(1)}$. The correspondence of orbital entanglement and static (or nondynamic) electron correlation permits the definition of such a diagnostic. We chose our diagnostic to meet important requirements such as well-defined limits for pure single-configurational and multi-configurational wave functions. The $Z_{s(1)}$ diagnostic can be evaluated from a partially converged, but qualitatively correct, and therefore inexpensive density matrix renormalization group wave function as in our recently presented automated active orbital selection protocol. Its robustness and the fact that it can be evaluated at low cost make this diagnostic a practical tool for routine applications.

Keywords: multi-configurational diagnostic, electron correlation, orbital entanglement, density matrix renormalization group

I. Introduction

The electronic structure of molecules is undoubtedly diverse and required the development of the plethora of quantum chemical methods applied today. Since there is not a single (feasible) method that allows calculations of sufficient accuracy for an arbitrary problem, the choice of a suitable approach stands at the beginning of each quantum chemical investigation. The classification according to the degree of static electron correlation of the wave function is of particular importance. Static electron correlation occurs when the wave function must be represented by more than one electronic configuration with considerable weight, while dynamic electron correlation is caused by the multitude of configurations with little weight in the total wave function. A robust diagnostic for the degree of static correlation is highly required.

Naturally, several such diagnostics were proposed to assist the selection of a suitable method for the problem under investigation. Among these is the T_1 -diagnostic,¹ which is defined as the Frobenius norm of the single-excitation amplitude vector of a coupled-cluster wave function with singles and doubles excitations divided by the square root of the number of correlated electrons. Closely related is the D_1 diagnostic, which is based on the matrix norm of the same single-excitation amplitude vector.² In addition to these diagnostics a density functional theory based diagnostic was proposed that quantifies the error introduced by the Hartree–Fock exchange in hybrid functionals, where it is known that Hartree–Fock exchange is inaccurate for multi-configurational systems.³

While these definitions all rely on a single-configurational wave function (that will be qualitatively wrong in

the multi-configurational regime), other diagnostics are obtained from multi-configurational wave functions. Among these are diagnostics based on natural orbital occupation numbers^{4,5} or the corresponding first-order reduced density matrix,⁶ and a diagnostic based on Monte Carlo configuration interaction (CI).⁷ A comprehensive review of these diagnostics including a comparison for several critical cases can be found in Ref. 8.

Another way to think about electron correlation is orbital entanglement derived from grand-canonical reduced density matrices.^{9–11} Orbital entanglement is directly related to static (or nondynamic) correlation¹² and permits us here to present a multi-configurational diagnostic based on these quantities. Although similar attempts have already been made,^{8,12–14} we show how a modified diagnostic based on the orbital entanglement overcomes the problems of these previous definitions. We furthermore show how the evaluation of this diagnostic can be incorporated in the algorithm of our recently proposed automated selection of active orbitals¹⁵ and can therefore be obtained at low cost.

This article is organized as follows: We first summarize properties we demand of a multi-configurational diagnostic and show how these requirements are met by an entanglement based criterion. Then, we show how this diagnostic can be easily obtained in the framework of our automated orbital selection protocol and study several critical cases.

^{a)}Corresponding author: markus.reiher@phys.chem.ethz.ch

II. Entanglement Based Multi-Configurational Diagnostic

A. Desirable properties

By definition, a "diagnostic" has to reveal the nature of a given problem (or an aspect thereof) such that suitable measures can be taken to solve the problem. Therefore, the main requirement for a multi-configuration diagnostic is the clear identification of strong static correlation that requires a multi-configuration description.

In this sense, well-defined limits are preferable and we require our measure to give a value of zero in the absence of electron correlation (i.e., when the wave function is exactly described by a single Slater determinant) and a value of one for strong static correlation. These well-defined limits facilitate the definition of a threshold value for the diagnostic below which single-configurational methods can safely be used whereas multi-configurational methods are necessary if the diagnostic gives a value above that threshold.

If the diagnostic is meant to guide the selection of a suitable method rather than only assess the quality of an already converged calculation, its evaluation should take only a small fraction of the total computational time. That a multi-configuration diagnostic should be obtained from a qualitatively correct multi-configurational wave function (that still includes single-configurational wave functions as limiting cases¹⁶) is an additional natural criterion.

B. Definition and constraints

Our multi-configuration diagnostic is based on the single-orbital entropy defined as^{9–11}

$$s_i(1) = - \sum_{\alpha=1}^4 \omega_{\alpha,i} \ln \omega_{\alpha,i}, \quad (1)$$

where the $\omega_{\alpha,i}$ are the eigenvalues of the one-orbital reduced density matrix for the i th orbital and α runs over the four possible occupations in a spatial orbital basis (doubly occupied, spin up, spin down, unoccupied). Maximum entanglement corresponds to a situation where all occupations are equally likely ($\omega_{\alpha,i} = 0.25$ for all α) and is therefore equal to $\ln 4 \approx 1.39$. This theoretical maximum allows for a scaling of the multi-configuration diagnostic $Z_{s(1)}$ such that correct limits as discussed above (0 = no entanglement, 1 = full entanglement) exist,

$$Z_{s(1)} = \frac{1}{L \ln 4} \sum_i^L s_i(1), \quad (2)$$

where L is the number of orbitals considered for the evaluation of $Z_{s(1)}$. This scaling allows us to compare the diagnostic between different active space sizes which was not the case for some previous definitions of entanglement based diagnostics.^{13,14} The single-orbital entropies

can easily be evaluated from a density matrix renormalization group (DMRG) wave function.^{17–31}

Maximum entanglement can only be realized if the number of electrons equals the number of spatial orbitals over which they are distributed and the number of orbitals is even. It is therefore necessary to restrict the set of orbitals whose single-orbital entropies define $Z_{s(1)}$ to the set of most entangled orbitals of a given calculation. If no such restriction is applied (as in Ref. 8), the large number of virtual orbitals will artificially lower $Z_{s(1)}$ because the four possible occupations cannot be realized with the electrons available in the system.

The identification of the most entangled orbitals of a given calculation is therefore crucial to define $Z_{s(1)}$ such that its values can be compared between different systems or orbital bases. This is also central to our recently proposed protocol for the automated selection of active orbital spaces for multi-configuration calculations.¹⁵ For the calculation of $Z_{s(1)}$ we may exploit the protocol of Ref. 15 for partially converged, qualitatively correct DMRG wave functions to identify a set strongly entangled orbitals. We then restrict the set of orbitals to fulfill the requirement that the number of electrons equals the number of orbitals and further exclude singly-occupied molecular orbitals (SOMOs) in open-shell cases. This special treatment of SOMOs is also a peculiarity of other multi-configuration diagnostics and justified by the observation that they are usually only weakly entangled.⁴ The diagnostic $Z_{s(1)}$ is then evaluated from this restricted set of orbitals. Within our automated selection protocol, we obtain the diagnostic for free as a byproduct of an initial, partially converged DMRG calculation with a large active space.

III. Computational methodology

We applied the ANO-RCC basis set^{32,33} in its double zeta contraction in combination with the Douglas-Kroll-Hess Hamiltonian at second order^{34–36} in all calculations. Initial orbitals were obtained with the complete active space self-consistent field (CASSCF) method as implemented in MOLCAS 8.³⁷ All DMRG calculations as well as the evaluation of $s(1)$ were performed with our DMRG program QCMAquis.^{38–40} For these calculations, we adopt the notation of Ref. 15: DMRG[m](N, L)#orbital_basis, where m is the number of renormalized states, N and L are the number of active electrons and orbitals, respectively, and the string after the hashtag specifies the orbital basis of the DMRG-CI calculations. With CAS(N, L)SCF, we adopt a very similar notation to specify the setup of the initial orbital generation. The number of sweeps was set to twelve in all DMRG calculations and the definition of a plateau in the threshold diagrams of our automated orbital selection procedure¹⁵ is set to ten. When $Z_{s(1)}$ is evaluated for wave functions from previously published studies, we refer to the original literature for the computational setup.

IV. Results

A. Bond stretching

In many cases the limit of almost pure dynamical correlation and strong static correlation can be realized by different structures of the same molecule. A prototype is the H_2 molecule, which has almost no static correlation in its equilibrium structure and becomes more and more statically correlated when the HH bond is elongated. A similar behavior is observed for the CC stretch coordinate in ethylene and the symmetric OO stretch in ozone although the degree of static correlation is higher already in the equilibrium structure of these molecules. Ref. 4 contains a diagram of the dependence of an occupation number based multi-configuration diagnostic on these stretch coordinates that we reproduce in FIG. 1 for $Z_{s(1)}$. The figure shows that $Z_{s(1)}$ is a continuous function

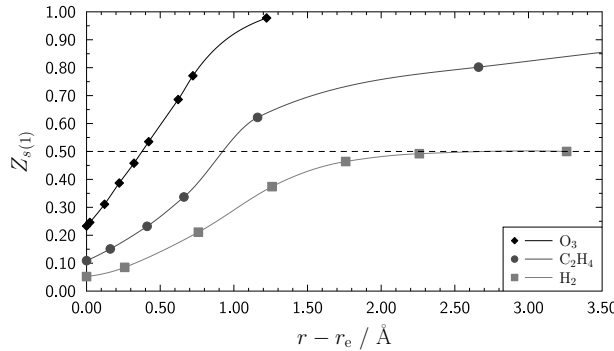


FIG. 1. Multi-configuration diagnostic $Z_{s(1)}$ as a function of the HH, CC, and symmetric OO bond elongation in H_2 , ethylene, and ozone, respectively. The equilibrium distances are chosen as in Ref. 4: $r_e(\text{HH}) = 0.741 \text{ \AA}$, $r_e(\text{CC}) = 1.339 \text{ \AA}$, and $r_e(\text{CC}) = 1.278 \text{ \AA}$. Internal coordinates that were kept fixed are: $r_e(\text{CH}) = 1.086 \text{ \AA}$, $\angle \text{HCH} = 117.6^\circ$, $\angle \text{HCC} = 121.2^\circ$, and $\angle \text{OOO} = 116.8^\circ$. The lines are produced from spline fits and meant to guide the eye.

with increasing distances and gives the right order of multi-configuration character at the equilibrium structure of these three molecules. The data in FIG. 1 is obtained from full-valence DMRG[500]-CI calculations with CAS(2,2)-SCF, CAS(4,4)-SCF, and CAS(6,9)-SCF initial orbitals for H_2 , ethylene, and ozone, respectively. The limit for $Z_{s(1)}$ is 0.5 in the case of H_2 because only two electrons are available and symmetry constraints of the molecular orbitals apply such that the theoretical limit for $s(1)$ becomes $\ln 2$.

B. Size independence

Independence of the size of the molecule or the active space is another criterion to be fulfilled by a multi-configuration diagnostic. In order to show that this holds true for $Z_{s(1)}$, we evaluated its value for methane, propane, and pentane from full-valence

DMRG[500]#CAS(4,4)SCF calculations. The initial four active orbitals were selected from around the Fermi level (i.e. HOMO-1, HOMO, LUMO, LUMO+1). In

TABLE I. Multi-configuration diagnostic $Z_{s(1)}$ for three alkane molecules from full-valence DMRG[500](N, L)#CAS(4,4)SCF calculations.

	methane	propane	pentane
active space (N, L)	(8,8)	(20,20)	(32,32)
$Z_{s(1)}$	0.04	0.03	0.03

all cases, the diagnostic has a very low value and is almost exactly the same for these three molecules with very similar electronic structure. We obtain identical results for calculations where convergence with respect to the energy is not reached in the case of propane and pentane. The active space selected by the automated procedure is the full-valence space. This is due to the fact that even the most entangled orbitals have a very low single-orbital entropy and a selection with respect to the maximum $s(1)$ value of a given calculation is prone to overestimate the number of active orbitals required. In these cases, a very low $Z_{s(1)}$ value can in the automated selection procedure¹⁵ point toward single-configuration methods, that are then a more appropriate choice.

C. Singlet vs. triplet wave functions

Often, the multi-configuration character of a wave function changes significantly with the spin state. A well-known example is the oxygen molecule that has a strong multi-configuration character in its singlet state, while a single Slater determinant is a qualitatively correct approximation to its triplet ground state. In CF_2 , this change of the multi-configuration character is much more subtle and in H_2CC , it is also less pronounced but the tendency is reversed. The data in Table II reveal that $Z_{s(1)}$ identifies very subtle differences in the multi-configuration nature of the wave function. The

TABLE II. Multi-configuration diagnostic $Z_{s(1)}$ for the singlet and triplet wave function of three molecules along with the weights of the largest CI coefficients from initial CASSCF calculations. Structures and active spaces for the initial CASSCF calculations were chosen as in Ref. 5.

molecule	singlet		triplet	
	$Z_{s(1)}$	weight	$Z_{s(1)}$	weight
O_2	0.37	45 %, 45 %	0.09	91 %
CF_2	0.10	95 %	0.09	96 %
H_2CC	0.10	93 %	0.16	92 %

information obtained agrees with that from the weights of the largest CI coefficients in the preceding CASSCF calculation, where weights that differ substantially from unity indicate multi-configuration character.¹ Note that the information of the weight of the largest CI

coefficient is not always available or reliable because the orbital basis is not necessarily obtained with CASSCF or with a too small active space.

D. Independence of orbital basis

In Ref. 15 we investigated the suitability of different orbital bases for the automated active space selection. Here, we examine how much the orbital basis influences the final value of $Z_{s(1)}$. We chose MnO_4^- with a Hartree–Fock, split-localized, CAS(10,10)SCF and DMRG[500](38,25)-SCF orbital basis as an example (see Ref. 15 for details about the computational setup).

TABLE III. Multi-configurational diagnostic $Z_{s(1)}$ for MnO_4^- obtained from full-valence DMRG-CI calculations employing different orbital bases.

basis	Hartree–Fock	split-localized	CAS(10,10)-SCF	DMRG[500](38,25)-SCF
$Z_{s(1)}$	0.27	0.31	0.32	0.34

The multi-configurational character is only slightly depending on the orbital basis. In Table III, the orbital bases are arranged in an increasingly optimized order and $Z_{s(1)}$ follows that trend by assigning an increasing multi-configurational character. This does not influence the performance of $Z_{s(1)}$ because the multi-configurational character is identified even for the wave function based on Hartree–Fock orbitals.

V. Conclusions

We presented a new orbital entanglement based multi-configurational diagnostic and applied it to several critical examples. Although a similar diagnostic has previously been proposed,⁸ our definition overcomes the lack of well-defined limits. It satisfies all criteria a multi-configurational diagnostic should meet, mostly by construction, as shown in the numerical examples. Furthermore, it can be evaluated as a by-product of our automated orbital selection protocol.¹⁵ There, it even serves for the assessment of the applicability of a multi-configurational method and directly guides the choice of a computational method. The fact that this diagnostic can be evaluated from partially converged and therefore inexpensive calculations makes it attractive for routine calculations.

A multi-configurational diagnostic is not only supposed to rank wave functions according to their multi-configurational character but should also give advice if a single- or multi-configurational method is appropriate for a given calculation. This means that threshold values need to be introduced that split the range of values that $Z_{s(1)}$ can take into regimes that can safely be treated by

a single-configurational method and those where multi-configurational methods are required.

Until today no fundamental threshold has been defined and all values suggested in the literature rely on experience. Based on the results of this paper and a re-evaluation of our recent work^{15,16} we recommend single-configurational methods when $Z_{s(1)}$ is between 0 and 0.1, whereas we advice to apply multi-configurational methods when this value lies between 0.2 and 1.0. This leaves an undefined region between 0.1 and 0.2, where no clear preference between the two kinds of methods can be deduced. Obviously, this regime has to be handled with special care since it may contain borderline cases where single-configurational methods fail unexpectedly. In many cases, wave functions with $0.1 < Z_{s(1)} < 0.2$ may be calculated with good accuracy by both types of methods. However, in our automated selection protocol¹⁵ we issue an automated warning if $Z_{s(1)}$ should fall in that regime.

Acknowledgments

This work was supported by the Schweizerischer Nationalfonds. C.J.S. gratefully acknowledges a Kékule fellowship from the Fonds der Chemischen Industrie.

References

- ¹T. J. Lee and P. R. Taylor, “A Diagnostic for Determining the Quality of Single-Reference Electron Correlation Methods,” *Int. J. Quantum Chem.* **36**, 199–207 (1989).
- ²C. L. Janssen and I. M. B. Nielsen, “New diagnostics for coupled-cluster and møller-plesset perturbation theory,” *Chem. Phys. Lett.* **290**, 423–430 (1998).
- ³U. R. Fogueri, S. Kozuch, A. Karton, and J. M. L. Martin, “A simple DFT-based diagnostic for nondynamical correlation,” *Theor. Chem. Acc.* **132**, 1291 (2012).
- ⁴O. Tishchenko, J. Zheng, and D. G. Truhlar, “Multireference model chemistries for thermochemical kinetics,” *J. Chem. Theory Comput.* **4**, 1208–1219 (2008).
- ⁵J. L. Bao, A. Sand, L. Gagliardi, and D. G. Truhlar, “Correlated-participating-orbitals pair-density functional method and application to multiplet energy splittings of main-group divalent radicals,” *J. Chem. Theory Comput.* (2016), 10.1021/acs.jctc.6b00569.
- ⁶P.-O. Löwdin, “Quantum theory of many-particle systems. i. physical interpretations by means of density matrices, natural spin-orbitals, and convergence problems in the method of configurational interaction,” *Phys. Rev.* **97**, 1474–1489 (1955).
- ⁷J. P. Coe, P. Murphy, and M. J. Paterson, “Applying Monte Carlo configuration interaction to transition metal dimers: Exploring the balance between static and dynamic correlation,” *Chem. Phys. Lett.* **604**, 46–52 (2014).
- ⁸J. P. Coe and M. J. Paterson, “Investigating multireference character and correlation in quantum chemistry,” *J. Chem. Theory Comput.* **11**, 4189–4196 (2015).
- ⁹Ö. Legeza and J. Sólyom, “Optimizing the Density-Matrix Renormalization Group Method Using Quantum Information Entropy,” *Phys. Rev. B* **68**, 195116 (2003).
- ¹⁰Ö. Legeza and J. Sólyom, “Two-site entropy and quantum phase transitions in low-dimensional models,” *Phys. Rev. Lett.* **96**, 116401 (2006).

¹¹J. Rissler, R. M. Noack, and S. R. White, "Measuring Orbital Interaction using Quantum Information Theory," *Chem. Phys.* **323**, 519–531 (2006).

¹²K. Boguslawski, P. Tecmer, O. Legeza, and M. Reiher, "Entanglement measures for single- and multireference correlation effects," *J. Phys. Chem. Lett.* **3**, 3129–3135 (2012).

¹³O. Legeza and J. Sólyom, "Quantum data compression, quantum information generation, and the density-matrix renormalization-group method," *Phys. Rev. B* **70**, 205118 (2004).

¹⁴K. Boguslawski, P. Tecmer, G. Barcza, Ö. Legeza, and M. Reiher, "Orbital entanglement in bond-formation processes," *J. Chem. Theory Comput.* **9**, 2959–2973 (2013).

¹⁵C. J. Stein and M. Reiher, "Automated Selection of Active Orbital Spaces," *J. Chem. Theory Comput.* **12**, 1760–1771 (2016).

¹⁶C. J. Stein, V. von Burg, and M. Reiher, "The delicate balance of static and dynamic electron correlation," *J. Chem. Theory Comput.* **12**, 3764–3773 (2016).

¹⁷S. R. White, "Density matrix formulation for quantum renormalization groups," *Phys. Rev. Lett.* **69**, 2863–2866 (1992).

¹⁸S. R. White, "Density-matrix algorithms for quantum renormalization groups," *Phys. Rev. B* **48**, 10345–10356 (1993).

¹⁹Ö. Legeza, R. Noack, J. Sólyom, and L. Tincani, "Applications of quantum information in the density-matrix renormalization group," *Lect. Notes Phys.* **739**, 653–664 (2008).

²⁰G. K.-L. Chan, J. J. Dorando, D. Ghosh, J. Hachmann, E. Neuscamman, H. Wang, and T. Yanai, "An introduction to the density matrix renormalization group ansatz in quantum chemistry," *Prog. Theor. Chem. Phys.* **18**, 49–65 (2008).

²¹G. K.-L. Chan and D. Zgid, "The density matrix renormalization group in quantum chemistry," *Annu. Rep. Comput. Chem.*, **5**, 149–162 (2009).

²²K. H. Marti and M. Reiher, "The density matrix renormalization group algorithm in quantum chemistry," *Z. Phys. Chem.* **224**, 583–599 (2010).

²³G. K.-L. Chan and S. Sharma, "The density matrix renormalization group in chemistry," *Ann. Rev. Phys. Chem.* **62**, 465 (2011).

²⁴K. H. Marti and M. Reiher, "New electron correlation theories for transition metal chemistry," *Phys. Chem. Chem. Phys.* **13**, 6750–6759 (2011).

²⁵U. Schollwöck, "The density-matrix renormalization group in the age of matrix product states," *Annals of Physics* **326**, 96 – 192 (2011).

²⁶Y. Kurashige, "Multireference electron correlation methods with density matrix renormalisation group reference functions," *Mol. Phys.* **112**, 1485–1494 (2014).

²⁷Wouters, Sebastian and Van Neck, Dimitri, "The density matrix renormalization group for ab initio quantum chemistry," *Eur. Phys. J. D* **68**, 272 (2014).

²⁸T. Yanai, Y. Kurashige, W. Mizukami, J. Chalupský, T. N. Lan, and M. Saitow, "Density matrix renormalization group for ab initio calculations and associated dynamic correlation methods: A review of theory and applications," *Int. J. Quantum Chem.* **115**, 283–299 (2015).

²⁹S. Szalay, M. Pfeffer, V. Murg, G. Barcza, F. Verstraete, R. Schneider, and Ö. Legeza, "Tensor product methods and entanglement optimization for ab initio quantum chemistry," *Int. J. Quantum Chem.* **115**, 1342–1391 (2015).

³⁰S. Knecht, E. D. Hedegård, S. Keller, A. Kovyrshin, Y. Ma, A. Muolo, C. J. Stein, and M. Reiher, "New approaches for ab initio calculations of molecules with strong electron correlation," *Chimia* **70**, 244–251 (2016).

³¹G. K.-L. Chan, A. Keselman, N. Nakatani, Z. Li, and S. R. White, "Matrix product operators, matrix product states, and ab initio density matrix renormalization group algorithms," *J. Chem. Phys.* **145**, 014102 (2016).

³²B. O. Roos, R. Lindh, P.-Å. Malmqvist, V. Veryazov, and P.-O. Widmark, "Main Group Atoms and Dimers Studied with a New Relativistic ANO Basis Set," *J. Phys. Chem. A* **108**, 2851–2858 (2004).

³³P.-O. Widmark, P.-Å. Malmqvist, and B. O. Roos, "Density matrix averaged atomic natural orbital (ano) basis sets for correlated molecular wave functions," *Theor. Chim. Acta* **77**, 291–306 (1990).

³⁴B. A. Hess, "Relativistic Electronic-Structure Calculations Employing a Two-Component No-Pair Formalism with External-Field Projection Operators," *Phys. Rev. A* **33**, 3742–3748 (1986).

³⁵M. Reiher and A. Wolf, "Exact Decoupling of the Dirac Hamiltonian. I. General Theory," *J. Chem. Phys.* **121**, 2037–2047 (2004).

³⁶M. Reiher and A. Wolf, "Exact Decoupling of the Dirac Hamiltonian. II. The Generalized Douglas-Kroll-Hess Transformation up to Arbitrary Order," *J. Chem. Phys.* **121**, 10945–10956 (2004).

³⁷F. Aquilante, J. Autschbach, R. K. Carlson, L. F. Chibotaru, M. G. Delcey, L. De Vico, I. Fdez. Galván, N. Ferré, L. M. Frutos, L. Gagliardi, M. Garavelli, A. Giussani, C. E. Hoyer, G. Li Manni, H. Lischka, D. Ma, P. Å. Malmqvist, T. Müller, A. Nenov, M. Olivucci, T. B. Pedersen, D. Peng, F. Plasser, B. Pritchard, M. Reiher, I. Rivalta, I. Schapiro, J. Segarra-Mart, M. Stenrup, D. G. Truhlar, L. Ungur, A. Valentini, S. Vancoillie, V. Veryazov, V. P. Vysotskiy, O. Weingart, F. Zapata, and R. Lindh, "Molcas 8: New capabilities for multiconfigurational quantum chemical calculations across the periodic table," *J. Comput. Chem.* **37**, 506–541 (2015).

³⁸M. Dolfi, B. Bauer, S. Keller, A. Kosenkov, T. Ewart, A. Kantian, T. Giamarchi, and M. Troyer, "Matrix product state applications for the ALPS project," *Comput. Phys. Commun.* **185**, 3430–3440 (2014).

³⁹S. Keller, M. Dolfi, M. Troyer, and M. Reiher, "An efficient matrix product operator representation of the quantum chemical hamiltonian," *J. Chem. Phys.* **143**, 244118 (2015).

⁴⁰S. Keller and M. Reiher, "Spin-adapted matrix product states and operators," *J. Chem. Phys.* **144**, 134101 (2016).